CrystEngComm

PAPER

View Article Online
View Journal | View Issue

Cite this: *CrystEngComm*, 2014, **16**, 441

Anatase and brookite TiO_2 with various morphologies and their proposed building block†

Min-Han Yang,[a] Po-Chin Chen,[b] Min-Chiao Tsai,[a] Ting-Ting Chen,[a] I-Chun Chang,[a] Hsin-Tien Chiu[b] and Chi-Young Lee*[a]

Received 31st August 2013,
Accepted 21st October 2013

DOI: 10.1039/c3ce41750f

www.rsc.org/crystengcomm

In this work, brookite TiO_2 has been synthesized by a simple hydrothermal approach using sodium titanate as a precursor in the presence of a sodium fluoride aqueous solution. The ratio of brookite and anatase TiO_2 can be tailored by the NaF concentration. In a concentrated NaF solution, high quality brookite TiO_2 was acquired. Pure anatase nanoparticles were obtained in only deionized water. Moreover, the morphology and size of brookite TiO_2 can be tailored by using various acid treated titanates which influence the stability of the building blocks and nucleation points of TiO_2. Micro-sized flower-like brookite, submicro-sized urchin-like brookite and brookite nanorods with anatase nanoparticles were obtained. The micro-sized flower-like brookite remains the same shape and phase even at 800 °C, whereas obvious grains were formed on the matrix with brookite, rutile and anatase mixture phases at 900 °C. On the other hand, as the submicro-sized urchin-like brookite was heated, a rutile phase appeared at 750 °C and 100% grain-like rutile was obtained at 900 °C.

Introduction

In nature, TiO_2 exists generally in three crystal phases which are rutile ($P4_2/mnm$), anatase ($I4_1/amd$) and brookite ($Pcab$). Owing to these different crystalline polymorphs of TiO_2, it has unique physical and chemical properties[1,2] which have a variety of applications in photocatalysts,[3–5] dye sensitized solar cells,[6,7] lithium ion storage[8,9] and electrochromic devices.[10] In general, the rutile phase has been synthesized in strong acidic solutions[11] or at high temperature conditions,[12] whereas anatase is obtained in neutral or alkaline solutions.[13,14] Compared with rutile and anatase TiO_2, getting a high quantity brookite phase is complicated and needs particular conditions, such as a specific precursor, pH value and additive.[15–20]

Recently, brookite nanorods were synthesized using titanium bis(ammonium lactate) dihydroxide (TALH) in the presence of a urea solution.[18] Brookite nanoflowers were synthesized with tetrabutyl titanate (TBOT) as a precursor in an ammonia and sodium salts mixed aqueous solution.[15,20] Pseudo-cube shaped brookite nanocrystals were synthesized using an oleate-modified hydrothermal method and a water-soluble titanium–glycolate as a precursor.[19] The aforementioned methods can obtain high quality brookite TiO_2 crystals, but mostly use titanium organic compounds as precursors. The organic pollutants and high cost precursors may limit the study of the physical and chemical behaviors of brookite TiO_2 and its applications.

In this investigation, we attempt to synthesize brookite TiO_2 by a simple hydrothermal approach using sodium titanate as a precursor in the presence of a sodium fluoride aqueous solution. The morphology and size tailored brookite TiO_2 was obtained by tuning the acid treated sodium titanate. The influence of the additive salts and dissolving rate of the precursors in the reaction on the brookite phase formation were discussed.

Experimental

Preparation of sodium titanate

Sodium titanate was synthesized by adding TiO_2 (Riedel-de-Haën) to a 10 M NaOH aqueous solution. The mixture was refluxed at 150 °C for 48 h. The obtained precipitates were washed with DI water several times to remove the unreacted NaOH. Furthermore, the sodium titanate was separated into four parts. The collected precipitates were suspended in DI water and underwent acidic treatments in which HCl was added until the solutions became invariable with respect to pH values at 8, 5, 4 or 2, respectively, for 24 h. The precipitates were further washed with DI water, dried at 50 °C and

[a] *Department of Materials Science and Engineering, National Tsing Hua University, Taiwan, Hsinchu, 30013, Republic of China. E-mail: cylee@mx.nthu.edu.tw; Fax: +886 3571 3113; Tel: +886 3572 8692*
[b] *Department of Applied Chemistry, National Chiao Tung University, Taiwan, Hsinchu, 300, Republic of China. E-mail: htchiu@cc.nctu.edu.tw; Fax: +886 3571 3113; Tel: +886 3513 1514*

† Electronic supplementary information (ESI) available. See DOI: 10.1039/c3ce41750f

then collected as precursors. The acid treated titanates were denoted as T8 (pH 8), T5 (pH 5), T4 (pH 4) and T2 (pH 2), respectively.

Preparation of TiO_2

0.2 g of the titanates (T8, T5, T4 or T2) were added to 30 ml (0 to 1 M) of a NaF solution under ultrasonication. The precursor solution was transferred to a Teflon-lined autoclave and heated to 200 °C for 20 h. After the hydrothermal process, the product was washed with DI water and dried in a 50 °C oven. For further confirmation, other salts (LiF, KF, NaCl and NaBr) were added individually or as a mixture of LiF and NaCl as well as KF and NaCl in the hydrothermal processes. To study the phase transformation, brookite TiO_2 was annealed at various temperatures (700 °C to 950 °C) for 1 h.

Materials characterization

The morphologies of the materials were examined by FE-SEM (JSE-6500F field emission SEM). The high resolution morphological analyses were performed by HRTEM (JEM-2010 and JEM-3000F). Phase detection analyses were studied by XRD patterns (Brucker D8-advanced with Cu K_α radiation, λ = 1.5405981 Å). A Raman spectrometer (Renishaw using a laser with λ = 632.8 nm) was used to characterize the structure of the samples. The trace element in the samples was identified by ICP-MS (Perkin Elmer, SCIEX ELAN 5000).

Quantitative analysis of the TiO_2 phase composition

The phase content of the TiO_2 polymorphs was estimated based on the integrated intensities of the anatase (101), brookite (121) and rutile (110). The weight fraction of TiO_2 can be derived:[21]

$$W_A = \frac{K_A A_A}{K_A A_A + K_B A_B + A_R}$$

$$W_B = \frac{K_B A_B}{K_A A_A + K_B A_B + A_R}$$

$$W_R = \frac{A_R}{K_A A_A + K_B A_B + A_R}$$

where W_A, W_B and W_R refer to the weight fraction of anatase, brookite and rutile, respectively. A_A, A_B and A_R represent the integrated intensities of the anatase (101) peak, brookite (121) peak and rutile (110) peak, respectively. K_A and K_B are two coefficients which are 0.886 and 2.721, respectively.

Results and discussion

TiO_2 with various amounts of brookite and anatase was synthesized using sodium titanate as the precursor in the presence of a NaF solution. Fig. 1 shows the XRD patterns of TiO_2 synthesized using T8 as a precursor in different concentrated NaF solutions. An anatase phase (JCPDS file no. 21-1272) was mainly obtained in only DI water (in the absence of NaF as the additive), whereas increasing the concentration of NaF leads to an increase in the 2θ peak at 30.8°, which corresponds to the reflection from the brookite TiO_2 lattice plane {121} (JCPDS file no. 29-1360). Raman spectra are also used to identify the phase structures.[22,23] Fig. S1 in the ESI† shows the Raman spectra of TiO_2 obtained in 0, 0.4 and 1 M NaF solutions, respectively. The peaks of TiO_2 obtained in DI water correspond to anatase phase TiO_2. The anatase and brookite overlapped peaks were observed in the spectrum of TiO_2 obtained in 0.4 M NaF. In the spectrum of TiO_2 obtained in 1 M NaF, brookite TiO_2 was the only product obtained, which was confirmed by the Ramen spectra, without significant anatase peaks (A_{1g} and B_{1g}) present at around 515 cm^{-1}. In addition, the XRD peaks at 9.3°, 24.2° and 28.2° correspond to the unreacted titanate precursor, as shown in Fig. 1 and Fig. S2 in the ESI.† It implies that the addition of NaF slows down the reaction rate and enhances the brookite formation.

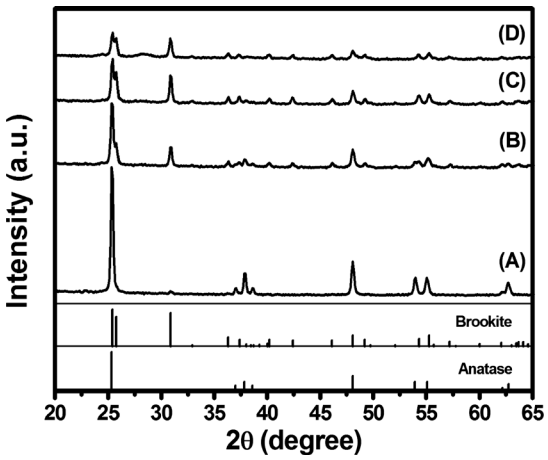

Fig. 1 Powder XRD patterns of TiO_2 obtained in (A) 0 M (B) 0.4 M (C) 0.6 M (D) 1 M NaF using T8 as a precursor in the hydrothermal process.

Fig. 2 shows the SEM images of TiO_2 synthesized using T8 as a precursor in NaF solutions with different concentrations. Fig. 2A shows irregular shaped particles which are hundreds of nanometres in size, obtained using DI water in the absence of NaF. A mixture of micro-sized flower shaped powder and particles was obtained in the reaction solution with respect to the addition of NaF, as shown in Fig. 2B and C. The content and size of the flower-like brookite increased as the NaF concentration increased. In a 1.0 M NaF solution, 4–5 μm sized flower-like brookite was covered by titanate nanowires, as shown in Fig. 2D and Fig. S3A in the ESI.† After a concentrated HCl treatment, the unreacted titanate was removed. High purity micro-sized flower-like brookite with a clean surface was obtained, as shown in Fig. S3B and S3C in the ESI.†

To investigate the role of the precursor on the brookite TiO_2 formation, the sodium titanate was washed using an HCl solution with different pH values to obtain titanates with

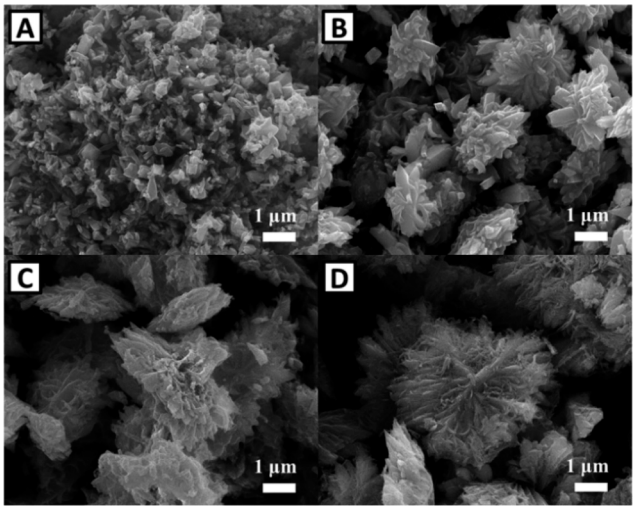

Fig. 2 FESEM images of TiO_2 obtained in (A) 0 M (B) 0.4 M (C) 0.6 M (D) 1.0 M NaF using T8 as a precursor in the hydrothermal process.

various displacement degrees of sodium by hydrogen ions. The sodium contents of the titanate decreased as they were acid treated in a solution with a lower pH value. From the EDS analysis shown in Fig. S4 in the ESI,† the Na/Ti ratio is 0.30, 0.24, 0.12 and 0.06 of T8, T5, T4 and T2, respectively. As a concentrated HCl solution was used, the sodium titanate is almost transferred to hydrogen titanate (T2). According to the literature,[24–27] this titanate is a $Na_xH_{2-x}Ti_3O_7{\cdot}nH_2O$ structure. The as-synthesized titanate was rich in sodium as an interlayer cation, but the sodium content was reduced substantially after an acidic treatment. In our experiments, some anatase peaks of T2 also can be discovered in Fig. S5 in the ESI.†

Fig. 3 shows the XRD patterns of TiO_2 using T5 as a precursor in different concentrations of NaF solutions. The peak intensities of brookite TiO_2 increased with the NaF concentration, as was observed using T8 as the precursor. The Raman spectrum in Fig. S6 in the ESI† also demonstrates that a high quantity of brookite TiO_2 was obtained in a 1 M NaF solution. On comparison with the sample made using T8, only TiO_2 peaks show on the XRD pattern when using T5 as a precursor in a 1 M NaF solution, which implies that T5 was totally consumed in a concentrated NaF solution, as shown in Fig. S7 in the ESI.†

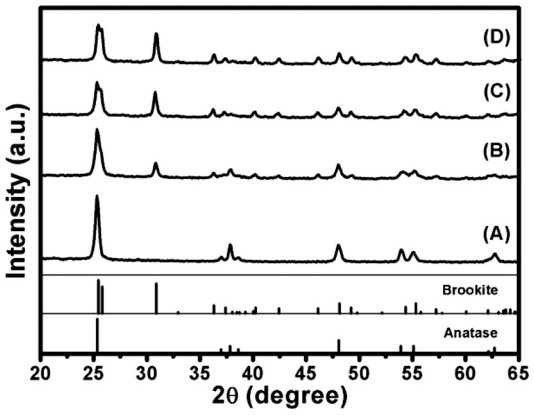

Fig. 3 Powder XRD patterns of TiO_2 obtained in (A) 0 M (B) 0.4 M (C) 0.6 M (D) 1 M NaF using T5 as a precursor in the hydrothermal process.

Fig. 4A–D shows the SEM images of TiO_2 obtained using T5 as a precursor in different concentrations of NaF solutions. Anatase TiO_2 nanoparticles, whose sizes are below 100 nm, are present in Fig. 4A. A mixture of submicro-sized brookite rods and anatase nanoparticles was observed with the use of NaF as an additive. The content of brookite rods increased with the NaF concentration. In a 1 M NaF solution, the urchin-like submicro-sized brookite was constructed with 400–500 nm length nanorods, which grow radially from the centre of the matrix. Fig. 4E shows low-magnification transmission electron microscopic images of the urchin-like brookite TiO_2, and Fig. 4F presents an HRTEM image of the top of the brookite nanorod. The fringes from the (120) and (001) planes reveal *d*-spacings of 3.51 Å and 5.15 Å, respectively. It shows that the rod axis of brookite is along [001] and the circumambient surface is the {120} planes.[28]

The XRD pattern shows mainly brookite phase TiO_2 obtained using T4 as a precursor in a 1 M NaF solution, as shown in Fig. 5A. As shown in Fig. 5B–F, uniform brookite nanorods with lengths of 200–300 nm and widths of 20–30 nm were obtained. In addition, a small amount of 10–20 nm anatase nanoparticles were also observed. Fig. 5D presents an HRTEM image of a brookite nanorod with

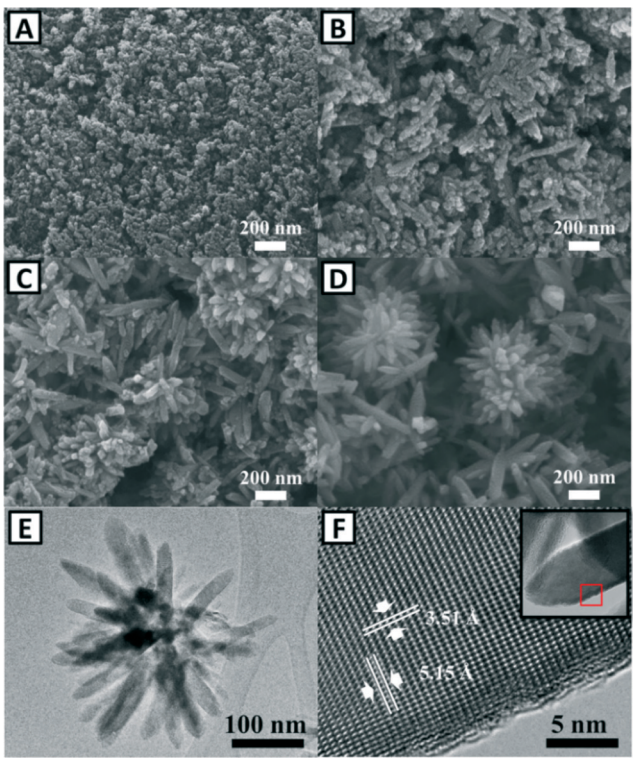

Fig. 4 FESEM images of TiO_2 obtained in (A) 0 M (B) 0.4 M (C) 0.6 M (D) 1 M NaF using T5 as a precursor in the hydrothermal process; TEM analyses of submicro-sized urchin-like brookite: (E) TEM image (F) HRTEM image of the red square in the inset.

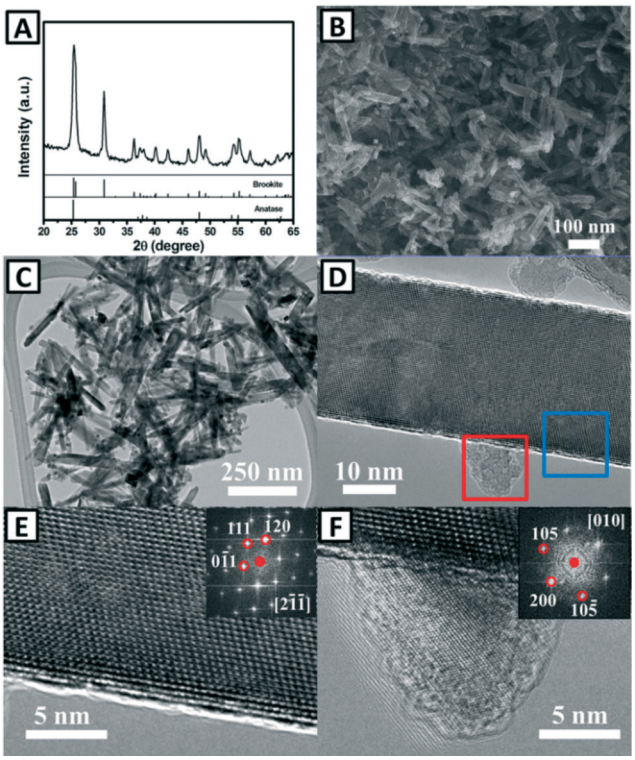

Fig. 5 TiO_2 obtained in 1 M NaF using T4 as a precursor in the hydrothermal process: (A) Powder XRD pattern (B) FESEM image. (C) and (D) shows TEM and HRTEM images of TiO_2. The marked blue and red regions in (D) are shown in (E) and (F) respectively. The insets of (E) and (F) present Fourier transformed images.

anatase nanoparticles. The spot patterns (inset of Fig. 5E) are a Fourier transformed image of the nanorod, assigned as brookite (120), $(0\bar{1}1)$ and (111) planes, whereas the spots (Fig. 5F) of the nanoparticle are indexed as the (200), (105) and $(10\bar{5})$ planes of anatase TiO_2.

Fig. 6A shows mainly anatase phase TiO_2 obtained using T2 as a precursor in a 1 M NaF solution. The size of the anatase nanoparticles was typically below 50 nm, as observed in Fig. 6B.

To further estimate the quantity of brookite TiO_2 thus obtained, the intensities of anatase (101) at 2θ = 25.3° and brookite (121) at 2θ = 30.8° were integrated,[21] as shown in Fig. 7. From Fig. 7, the phase content of TiO_2 using T8 and T5 as precursors shows a similar tendency. The amount of

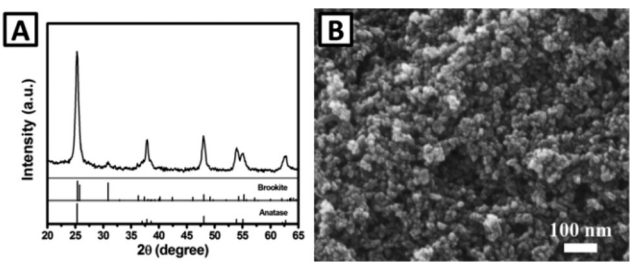

Fig. 6 TiO_2 obtained in 1 M NaF using T2 as a precursor in the hydrothermal process: (A) Powder XRD pattern (B) FESEM image.

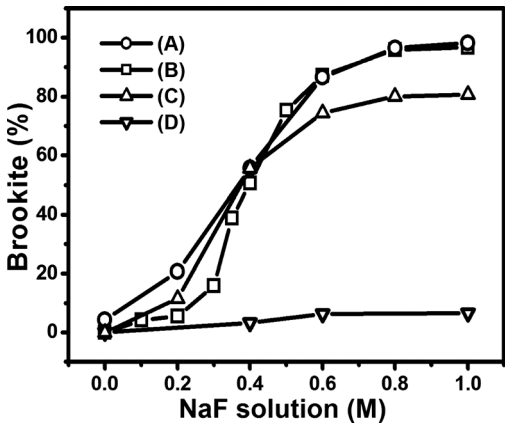

Fig. 7 The content of brookite TiO_2 obtained in different NaF concentrations using (A) T8, (B) T5, (C) T4 and (D) T2 as precursors in the hydrothermal process.

brookite increases dramatically as the concentration of the NaF solution increases from 0.2 M to 0.6 M and reaches over 95% in a 1 M NaF solution. When using T4 as a precursor, although the content of brookite increases as the concentration of the NaF solution increases from 0.2 M to 0.6 M, only 81% brookite was observed in 1 M NaF. However, the use of T2 as a precursor yields only 7% brookite TiO_2 in a 1 M NaF solution.

In addition to the use of different precursors, the reaction environment was also adjusted by different pH values. As T8 was suspended in a 1 M NaF acidic solution (pH 5), the product without unreacted titanate containing 68.4% brookite and 31.6% anatase was obtained, as shown in Fig. 8A. Reducing the pH value of the reaction solution accelerates the transformation of titanate to TiO_2, which diminishes the formation of brookite TiO_2 from 98% to 68.4%, and the size of the flower-like brookite also decreases to 2–3 μm.

Based on the above observations, micro-sized flower-like brookite with some unreacted titanate, submicro-sized urchin-like brookite, brookite nanorods with anatase nanoparticles and anatase nanoparticles were obtained using T8, T5, T4 and T2 as precursors, respectively, in a 1 M NaF solution. The results show that the size of the brookite lessened and the content of anatase increased as the sodium content in the titanate precursor decreased from T8 to T2.

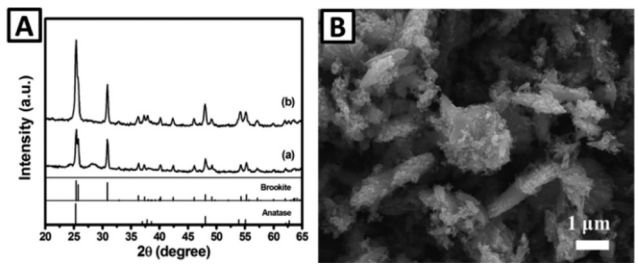

Fig. 8 (A) Powder XRD patterns of TiO_2 obtained (a) without HCl (b) with the addition of HCl and using T8 as a precursor in 1 M NaF (B) FESEM image of (b).

The size variation of brookite can be attributed to the dissolving rate of titanate. The weak acid treated T8, with a large amount of sodium ions, stabilizes the layered structure of titanate.[26] A low dissolving rate leads to the formation of large TiO_2 particles and retains some unreacted titanate.[29] However, on using a strong acid treated titanate, T2, or adding extra hydrochloric acid to the reaction solution, accelerates the titanate dissolution, which increases the nucleation sites, resulting in the formation of small sized TiO_2.[30,31] These observations also imply that when using a titanate with a high dissolution rate, anatase TiO_2 was the major product, whereas, brookite was obtained when the titanate dissolving rate is slow.

Moreover, various alkali metal halides were used to study the influence of salts on the TiO_2 growth. Sodium halides, NaCl and NaBr, which provide the sodium ion, and the alkali metal fluorides, LiF or KF, which provide the fluoride ion in the reaction, were used as additives. It was discovered that anatase TiO_2 powder without any other TiO_2 phase was obtained, as shown in Fig. S8 in the ESI.† These results suggest that both the sodium and fluoride ions are essential species for the formation of brookite TiO_2. When a mixture of equal molar KF and NaCl was used, 27% brookite TiO_2 was observed. However, when a mixture of LiF and NaCl was added in the reaction, only 5% brookite TiO_2 was obtained, as shown in Fig. 9.

Depending on the above observations, brookite TiO_2 was synthesized using a weak acid treated titanate as the precursor in NaF solutions. The brookite building block formed in a medium basic solution can be stabilized by coexisting ions of sodium and fluoride in the reaction,[32] which is unstable in the presence of other ions. The different contents of brookite TiO_2 in the mixed salt reactions may be attributed to the competition between various charge densities of the alkali metal ions.[14,33] As low charge density potassium ions were introduced, a portion of the brookite building blocks were still stabilized by the sodium ions, resulting in partial brookite TiO_2 formation. However, when the mixture of LiF and NaCl was added, high charge density lithium ions were introduced to replace most of the sodium ions, which can stabilize the brookite building block and lessen the formation of brookite TiO_2.

According to the titanate structure, $Na_xH_{2-x}Ti_3O_7{\cdot}nH_2O$,[34] the basic building blocks of TiO_2 could be examined. As titanates slowly dissolve in a concentrated NaF solution, the large building blocks of brookite TiO_2 can be stabilized in the process, resulting in brookite TiO_2 formation. On the other hand, titanates which dissolve very fast form small building units of TiO_2 in acidic solutions, resulting in the formation of anatase TiO_2, as shown in Scheme 1. Owing to the slow dissolution of titanate, some unreacted titanate still remained and a small amount of nucleation points of TiO_2 were generated in the beginning, leading to the formation of large sizes of brookite. However, when the titanates rapidly dissolved, the structure was decomposed immediately and generated small building units of TiO_2. The building blocks of brookite are damaged, causing the low content of brookite TiO_2. Because of the fast dissolution of titanate, a large amount of nucleation points of TiO_2 were generated in the beginning, leading to the formation of small sized TiO_2. Moreover, the NaF solution plays a key factor in stabilizing the building blocks of brookite. When the concentration of the NaF solution increased, a higher content of brookite was obtained by the stabilized building block of brookite. However, the other salts substitute for the NaF and the building blocks of brookite are unstable, leading to anatase, another phase of TiO_2, formation.

To study the phase transformation, micro-sized flower-like brookite and submicro-sized urchin-like brookite were annealed at various temperatures for 1 h, as shown in Fig. 10 and Fig. S9 in the ESI.† The micro-sized flower-like brookite retains its shape and phase even at 800 °C, whereas obvious grains were formed on the matrix with the brookite (12%), rutile (26%) and anatase (62%) phase mixtures at 900 °C (Fig. S10A–C, ESI†). On the other hand, as the submicro-sized urchin-like brookite was heated, a rutile phase appeared at

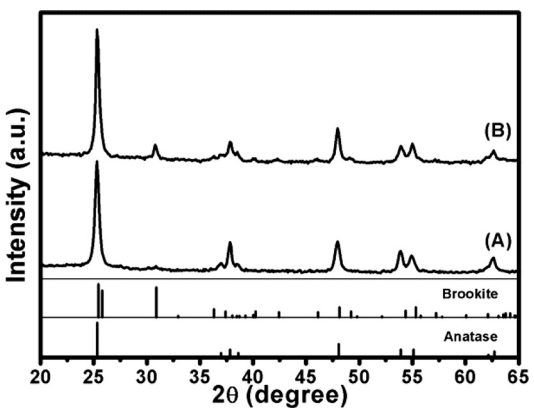

Fig. 9 Powder XRD patterns of TiO_2 obtained in the presence of a mixture of (A) LiF and NaCl, and (B) KF and NaCl solutions using T5 as a precursor in the hydrothermal process.

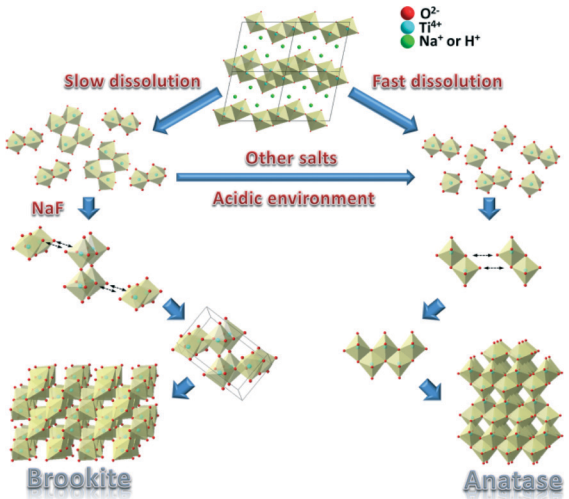

Scheme 1 The schematic representation of the TiO_2 crystal growth pathway.

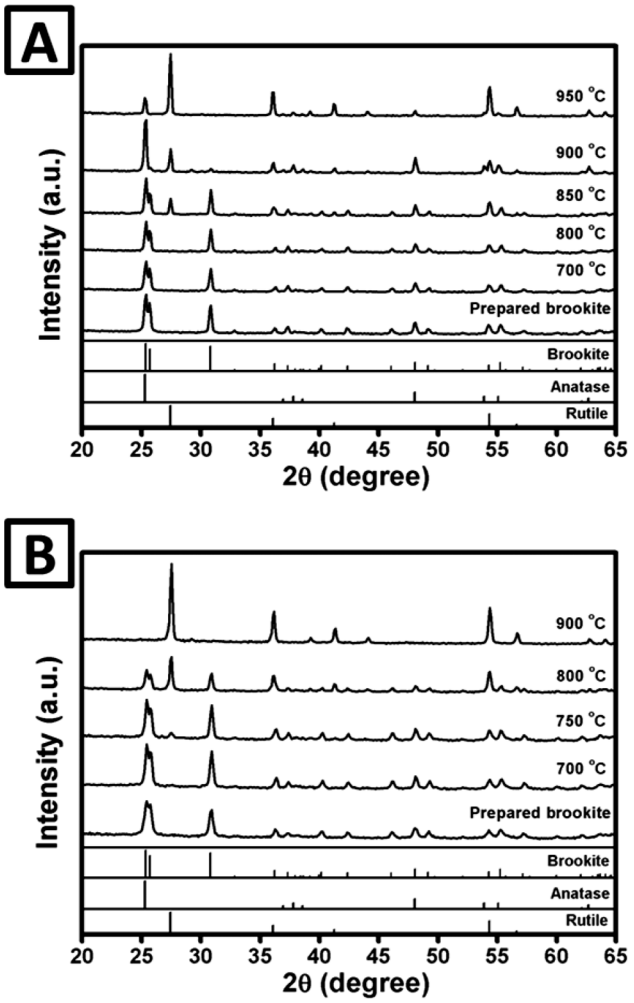

Fig. 10 Powder XRD patterns of (A) micro-sized flower-like brookite and (B) submicro-sized urchin-like brookite annealed at various temperatures for 1 h.

750 °C, about 40% rutile was obtained at 800 °C, and 100% grain rutile was obtained at 900 °C (Fig. S10D–F, ESI†). The Raman spectra also present a similar tendency for TiO_2 phase transformation at different temperatures in Fig. S11.†[22,23] The high thermal stability of micro-sized flower-like brookite may involve two aspects: the crystalline size of brookite TiO_2 and the Na content in brookite TiO_2. According to the literature,[21,35] brookite nanoparticles with diameters below 10 nm can undergo phase transformation above 500 °C, whereas 40 nm brookite nanoparticles are thermally stable up to 700 °C and transform to a rutile phase at 800 °C. The high thermal stability of micro-sized flower-like brookite may be attributed to the large crystalline size which stabilizes the brookite structure and avoids phase transformation.

On the other hand, it was reported that the impurities in the TiO_2 structure can affect the phase transformation temperature.[36] From the ICP analyses, there are trace Na ions remaining in the brookite TiO_2. The Na content or Na/Ti ratio in micro-sized flower-like brookite TiO_2 is slightly higher than that of submicro-sized urchin-like brookite. (Micro-sized flower-like brookite: 56.02% for Ti and 0.311% for Na; submicro-sized urchin-like brookite: 57.05% for Ti and 0.255% for Na). The Na ions in the micro-sized flower-like brookite may act as a stabilizer to retain its structure and raise the phase transformation temperature.

Conclusions

In summary, brookite TiO_2 was synthesized by a hydrothermal process using titanate as the precursor in the presence of NaF solutions. The content of brookite increased dramatically from 0.2 M to 0.6 M NaF solutions and to over 95% in a 1 M NaF solution. The morphology and size of brookite TiO_2 can be further tuned by using different acid treated titanates as the precursors. Micro-sized flower-like brookite with some unreacted titanate was obtained by using a weak acid treated titanate (T8). By using a middle acid treated titanate (T5), submicro-sized urchin-like brookite was acquired. Brookite nanorods with some anatase nanoparticles were achieved by using a strong acid treated titanate (T4). The titanate dissolving rate and brookite TiO_2 formation were further examined by adding an HCl solution to accelerate the T8 dissolving rate, which demonstrated that more anatase nanoparticles were obtained in the more acidic solution. Moreover, the high quality brookite TiO_2 can only be obtained in the presence of both sodium and fluoride ions. These observations reveal that the building blocks of brookite were generated by the slow dissolving titanate and stabilized in a NaF solution. The study of the phase transformation at various temperatures showed that the micro-sized flower-like brookite retains its shape and phase even at 800 °C, whereas obvious grains were formed on the matrix with the brookite, rutile and anatase mixture phases at 900 °C. On the other hand, as the submicro-sized urchin-like brookite was heated, a rutile phase appeared at 750 °C and 100% grain-like rutile was obtained at 900 °C. This research provides a systematic, low cost and green strategy for synthesizing size- and morphology-tailored brookite TiO_2. The method has a high potential for providing brookite TiO_2 in order to study its physical and chemical behaviours.

Acknowledgements

The authors would like to thank the National Science Council of the Republic of China, Taiwan, for financially supporting this research under contract no. NSC 101-2113-M-007-012-MY3.

Notes and references

1 S. D. Mo and W. Y. Ching, *Phys. Rev. B: Condens. Matter*, 1995, **51**, 13023.
2 R. Asahi, T. Morikawa, T. Ohwaki, K. Aoki and Y. Taga, *Science*, 2001, **293**, 269.
3 M.-H. Yang, P.-C. Chen, M.-C. Tsai, T.-T. Chen, I. C. Chang, H.-T. Chiu and C.-Y. Lee, *CrystEngComm*, 2013, **15**, 2966.

4 P.-C. Chen, M.-C. Tsai, M.-H. Yang, T.-T. Chen, H.-C. Chen, I. C. Chang, Y.-C. Chang, Y.-L. Chen, I. N. Lin, H.-T. Chiu and C.-Y. Lee, *Appl. Catal., B*, 2013, **142–143**, 752.
5 M. H. Yang, M. C. Tsai, Y. W. Chang, Y. C. Chang, H. T. Chiu and C. Y. Lee, *ChemCatChem*, 2013, **5**, 1871.
6 B. Oregan and M. Gratzel, *Nature*, 1991, **353**, 737.
7 B. Liu and E. S. Aydil, *J. Am. Chem. Soc.*, 2009, **131**, 3985.
8 Y. S. Hu, L. Kienle, Y. G. Guo and J. Maier, *Adv. Mater.*, 2006, **18**, 1421.
9 P. C. Chen, M. C. Tsai, H. C. Chen, I. N. Lin, H. S. Sheu, Y. S. Lin, J. G. Duh, H. T. Chiu and C. Y. Lee, *J. Mater. Chem.*, 2012, **22**, 5349.
10 M. H. Yang, T. T. Chen, Y. S. Wang, H. T. Chiu and C. Y. Lee, *J. Mater. Chem.*, 2011, **21**, 18738.
11 T. Y. Ke, C. W. Peng, C. Y. Lee, H. T. Chiu and H. S. Sheu, *CrystEngComm*, 2009, **11**, 1691.
12 T. Mitsuhashi and O. J. Kleppa, *J. Am. Ceram. Soc.*, 1979, **62**, 356.
13 T. Sugimoto, X. Zhou and A. Muramatsu, *J. Colloid Interface Sci.*, 2002, **252**, 339.
14 M. H. Yang, P. C. Chen, M. C. Tsai, T. T. Chen, I. C. Chang, H. T. Chiu and C. Y. Lee, *CrystEngComm*, 2013, **15**, 2966.
15 B. Zhao, F. Chen, Y. C. Jiao and J. L. Zhang, *J. Mater. Chem.*, 2010, **20**, 7990.
16 W. B. Hu, L. P. Li, G. S. Li, C. L. Tang and L. Sun, *Cryst. Growth Des.*, 2009, **9**, 3676.
17 H. F. Lin, L. P. Li, M. L. Zhao, X. S. Huang, X. M. Chen, G. S. Li and R. C. Yu, *J. Am. Chem. Soc.*, 2012, **134**, 8328.
18 T. A. Kandiel, A. Feldhoff, L. Robben, R. Dillert and D. W. Bahnemann, *Chem. Mater.*, 2010, **22**, 2050.
19 Y. Ohno, K. Tomita, Y. Komatsubara, T. Taniguchi, K. Katsumata, N. Matsushita, T. Kogure and K. Okada, *Cryst. Growth Des.*, 2011, **11**, 4831.
20 B. Zhao, F. Chen, Q. W. Huang and J. L. Zhang, *Chem. Commun.*, 2009, 5115.
21 H. Z. Zhang and J. F. Banfield, *J. Phys. Chem. B*, 2000, **104**, 3481.
22 G. A. Tompsett, G. A. Bowmaker, R. P. Cooney, J. B. Metson, K. A. Rodgers and J. M. Seakins, *J. Raman Spectrosc.*, 1995, **26**, 57.
23 U. Balachandran and N. G. Eror, *J. Solid State Chem.*, 1982, **42**, 276.
24 O. P. Ferreira, A. G. Souza, J. Mendes and O. L. Alves, *J. Braz. Chem. Soc.*, 2006, **17**, 393.
25 E. Morgado, M. A. S. de Abreu, O. R. C. Pravia, B. A. Marinkovic, P. M. Jardim, F. C. Rizzo and A. S. Araujo, *Solid State Sci.*, 2006, **8**, 888.
26 X. M. Sun and Y. D. Li, *Chem.–Eur. J.*, 2003, **9**, 2229.
27 E. Morgado, M. A. S. de Abreu, G. T. Moure, B. A. Marinkovic, P. M. Jardim and A. S. Araujo, *Chem. Mater.*, 2007, **19**, 665.
28 M. Zhao, L. Li, H. Lin, L. Yang and G. Li, *Chem. Commun.*, 2013, **49**, 7046.
29 I. C. Chang, P. C. Chen, M. C. Tsai, T. T. Chen, M. H. Yang, H. T. Chiu and C. Y. Lee, *CrystEngComm*, 2013, **15**, 2363.
30 D. V. Bavykin, J. M. Friedrich, A. A. Lapkin and F. C. Walsh, *Chem. Mater.*, 2006, **18**, 1124.
31 M. Qamar, C. R. Yoon, H. J. Oh, D. H. Kim, J. H. Jho, K. S. Lee, W. J. Lee, H. G. Lee and S. J. Kim, *Nanotechnology*, 2006, **17**, 5922.
32 H. Y. Yang, F. Chen, Y. C. Jiao and J. L. Zhang, *Chem.–Eur. J.*, 2013, **214**, 229.
33 R. D. Shannon, *Acta Crystallogr., Sect. A: Cryst. Phys., Diffr., Theor. Gen. Crystallogr.*, 1976, **32**, 751.
34 S. Andersson and A. D. Wadsley, *Acta Crystallogr.*, 1961, **14**, 1245.
35 T. A. Kandiel, L. Robben, A. Alkaim and D. Bahnemann, *Photochem. Photobiol. Sci.*, 2013, **12**, 602.
36 J. Choi, H. Park and M. R. Hoffmann, *J. Phys. Chem. C*, 2010, **114**, 783.